(4) (a) M. W. Bishop, J. Chatt, J. R. Dilworth, G. Kaufman, S. Kim, and J. Zubieta, *J. Chem. Soc., Chem. Commun.*, 70 (1977); (b) M. W. Bishop, J. Chatt, J. R. Dilworth, S. Kim, K. Venkatasubramanian, and J. Zubieta, *Inorg. Chem.*, **17**, 2917 (1978).
(5) J. Chatt, and J. R. Dilworth, *J. Less-Common Met.*, 36 (1974).
(6) (a) R. Eisenberg and J. A. Ibers, *J. Am. Chem. Soc.*, **87**, 3776 (1965); (b) *Inorg. Chem.*, **5**, 411 (1966).
(7) (a) R. Eisenberg, E. I. Steifel, R. C. Rosenberg, and H. B. Gray, *J. Am. Chem. Soc.*, **88**, 2874 (1966); (b) R. Eisenberg and H. B. Gray, *Inorg. Chem.*, **6**, 1844 (1967).
(8) M. J. Bennett, M. Cowie, J. L. Martin, and J. Takats, *J. Am. Chem. Soc.*, **95**, 7504 (1973).
(9) A. E. Smith, G. N. Schrauzer, V. P. Mayweg, and W. Heinrich, *J. Am. Chem. Soc.*, **87**, 5798 (1965).
(10) (a) E. I. Steifel, Z. Dori, and H. B. Gray, *J. Am. Chem. Soc.*, **89**, 3353 (1967); (b) G. F. Brown and E. I. Steifel, *Inorg. Chem.*, **12**, 2140 (1973).
(11) R. Eisenberg, *Prog. Inorg. Chem.*, **12**, 295 (1970).
(12) The crystallographic programs employed in the structure solution and refinement were those compiled in the 1972 version of the X-ray system described by J. M. Stewart, G. J. Kruger, H. L. Ammon, C. Dickinson, and S. R. Hall, Technical Report TR-192, University of Maryland, June 1972.
(13) "International Tables for X-ray Crystallography", Vol. III, Kynoch Press, Birmingham, England, pp 202, 204.
(14) E. L. Muetterties and L. J. Guggenberger, *J. Am. Chem. Soc.*, **96**, 1748 (1974).
(15) C. G. Pierpont and R. Eisenberg, *J. Chem. Soc. A*, 2285 (1971).
(16) R. Hoffmann, J. M. Howell, and A. R. Rossi, *J. Am. Chem. Soc.*, **98**, 2484 (1976).
(17) L. H. Jensen, *J. Am. Chem. Soc.*, **76**, 4663 (1954).
(18) E. N. Maslen, C. L. Paston, B. W. Skelton, and A. H. White, *Aust. J. Chem.*, **28**, 739 (1975).
(19) R. J. Baker, S. C. Nyburg, and J. T. Szymanski, *Inorg. Chem.*, **10**, 138 (1971).
(20) (a) P. Domiano, G. Fava Gaspari, M. Nardelli, and P. Sgarabotto, *Acta Crystallogr., Sect. B*, **25**, 343 (1969); (b) G. D. Andreetti, P. Domiano, G. Fava Gaspari, M. Nardelli, and P. Sgarabotto, *ibid.*, **26**, 1005 (1970).
(21) R. Groenback and S. E. Rasmussen, *Acta Chem. Scand.*, **16**, 2325 (1962).
(22) L. Cavalca, M. Nardelli, and G. Fava, *Acta Crystallogr.*, **15**, 1139 (1962).
(23) J. Finster, N. Meusel, P. Mullër, W. Dietzach, A. Meisel, and E. Hoyer, *Z. Chem.*, **13**, 146 (1973).
(24) (a) E. I. Steifel, *Proc. Natl. Acad. Sci. U.S.A.*, **70**, 988 (1973); (b) E. I. Steifel and J. K. Gardner, *J. Less-Common Met.*, **36**, 521 (1974).
(25) M. Cowie and M. J. Bennett, *Inorg. Chem.*, **15**, 1595 (1976).
(26) M. Cowie and M. J. Bennett, *Inorg. Chem.*, **15**, 1589 (1976).
(27) M. Cowie and M. J. Bennett, *Inorg. Chem.*, **15**, 1584 (1976).
(28) K. A. Jensen and C. Pedersen, *Acta Chem. Scand.*, **15**, 1097 (1961).
(29) G. Butler, J. Chatt, G. J. Leigh, and C. J. Pickett, unpublished results.
(30) E. I. Steifel and J. R. Gardner, *J. Less-Common Met.*, **36**, 521 (1974).
(31) L. Pauling, "The Nature of the Chemical Bond", 3rd ed., Cornell University Press, Ithaca, N.Y., 1960.

Contribution from the Department of Chemistry,
The University of Chicago, Chicago, Illinois 60637

Crystal and Molecular Structure of the Five-Coordinate Mn(III) Macrocyclic Complex (7,16-Dihydro-6,8,15,17-tetramethyldibenzo[*b*,*i*][1,4,8,11]tetraazacyclotetradecinato)-(isothiocyanato)manganese(III)

MARVIN C. WEISS and VIRGIL L. GOEDKEN*[1]

Received August 4, 1978

The crystal and molecular structure of the high-spin, five-coordinate Mn(III) complex [Mn($C_{22}H_{22}N_4$)(NCS)] containing the dibenzotetraaza[14]annulene macrocyclic ligand 7,16-dihydro-6,8,15,17-tetramethyldibenzo[*b*,*i*][1,4,8,11]tetraazacyclotetradecinato has been determined from three-dimensional X-ray diffraction data. The complex crystallizes in the orthorhombic space group $D_{2h}{}^{14}$-*Pbcn* with the cell dimensions a = 14.678 (4), b = 8.704 (2), and c = 16.093 (4) Å with Z = 4, each molecule lying on a crystallographic dyad. The structure was refined by Fourier and least-squares techniques to conventional and weighted R values of 0.041 and 0.054, respectively, based on 1999 data with $|F_o| \geq 3\sigma(F_o)$. The average Mn(III)–N(macrocycle) bond distance is 1.958 (6) Å, while the Mn(III)–N(axial) bond distance is 2.115 (4) Å. The Mn(III) is displaced by 0.356 Å from the N_4 donor plane, and the macrocyclic ligand has the usual saddle conformation. Comparisons are made with related Mn(III) structures containing porphyrin, macrocyclic, and tetradentate ligands as well as with other five-coordinate complexes containing the title macrocycle.

Introduction

In the not too distant past, stable Mn(III) complexes were thought to be confined largely to the oxides.[2] The more notable exceptions were Mn(III) complexes of acetate, 2,4-pentanedione, and a few Schiff bases—all of which are strong oxidants.[3-5] More recently, it has been found that Mn(III) can be generated chemically[6] or electrochemically[7] with a number of ligands, particularly macrocyclic ligands, and that for some of these, especially porphyrins, Mn(III) appears to be the preferred oxidation state. It must be concluded that Mn(III) is not an uncommon oxidation state and considerably more effort is warranted in elucidating its structural and reactivity preferences.

A five-coordinate square-pyramidal geometry has been shown to be the preferred stereochemistry for the simple complexes of the dihydro-6,8,15,17-tetramethyldibenzo-[*b*,*i*][1,4,8,11]tetraazacyclotetradecinato ligand, I. The preponderance of structural data suggests that the ligand induces, partially as a consequence of its steric interactions, a tendency toward five-coordination with a preference for the metal to be displaced from the macrocyclic N_4 plane. As described previously,[9-11] the saddle conformation of the ligand allows maximum bonding interactions while minimizing the peripheral steric interactions: (1) maximization of overlap between the N(equatorial) lone-pair electrons with the appropriate metal orbitals, (2) maintenance of planarity in the 2,4-pentanediiminato chelate rings, and (3) relief of steric interaction at the periphery.

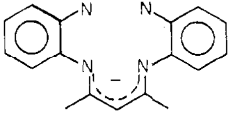

I

The structure of the title complex was determined as part of our program of studying the relationships between the structure and reactivity patterns of I with a number of first- and second-row transition metals The structural parameters associated with the Mn(III) complex are expected to be consistent with the systematic trend of values established by the study of the Mn(II), Fe(III), and Co(III) five-coordinate complexes containing the same macrocyclic ligand. Thus the structure of [Mn($C_{22}H_{22}N_4$)(NCS)] is discussed in light of the previous results obtained for [Mn($C_{22}H_{22}N_4$)(N(C_2H_5)$_3$)], [Fe($C_{22}H_{22}N_4$)Cl], and [Co($C_{22}H_{22}N_4$)I]. Comparisons are made with other five- and six-coordinate high-spin Mn(III) complexes, especially the porphyrin counterparts [Mn(TPP)Cl][12-14] and [Mn(TPP)N_3].[12] Some contrasts are noted

Table I. Crystal Data for $[Mn(C_{22}H_{22}N_4)(NCS)]$

mol wt	455.46
space group	*Pbcn*
cell constants	
a, Å	14.678 (4)
b, Å	8.704 (2)
c, Å	16.093 (4)
V, Å^3	2056.09
no. of reflections used to determine cell constants and their 2θ limits, deg	30; $35 < 2\theta < 45$
Z	4
ρ_{calcd}, g cm^{-3}	1.471
ρ_{exptl}, g cm^{-3}	1.48
μ, cm^{-1}	7.90

concerning the inner coordination geometry in the five-coordinate Mn(III) porphyrins.

Experimental Section

Synthesis of $[Mn(C_{22}H_{22}N_4)(NCS)]$. The free ligand was prepared as previously described. The Mn(III) complex was prepared by a modification of the procedure reported by Dabrowiak et al.[7] One equivalent of bis(*o*-phenylenediamine)bis(thiocyanato)manganese(II) and 1 equiv of the free ligand were stirred, as a suspension in dry acetonitrile under nitrogen, and then 4 equiv of degassed anhydrous triethylamine was added. The five-coordinate complex $[Mn(C_{22}H_{22}N_4)(N(C_2H_5)_3)]$ formed while the reaction vessel was gently heated at 50 °C for 5 min. A 22-gauge needle was then inserted through a serum cap mounted on one arm of the vessel, and the apparatus was cooled to 0 °C. The solution immediately turned from red-brown to dark green with the addition of air, and the product slowly crystallized from solution over a 2-h period. The air-stable compound was filtered, washed with acetonitrile, and dried in vacuo. The analytical data, magnetic susceptibility ($\mu = 4.97\ \mu_B$), and electronic absorption spectra were identical with that reported by Dabrowiak.

Well-formed crystals suitable for X-ray diffraction studies were isolated from aerially "decomposed" acetonitrile solutions of $[Mn(C_{22}H_{22}N_4)(N(C_2H_5)_3)]$ containing NaNCS. X-ray-quality crystals were also obtained by the reported procedure utilizing the Mn(III) precursor complex $[Mn(acac)_2NCS]$ and the free ligand.

Electronic Spectra. The solution spectra were taken in a chloroform solution under a nitrogen atmosphere; the solid-state spectra were taken by mulling the powdered complex in mineral oil (Nujol) between KBr plates.

Crystal Examination and Data Collection. Crystals suitable for X-ray diffraction studies were obtained by slow crystal growth from the crude reaction mixture. A crystal with dimensions 0.5 × 0.3 × 0.35 mm was selected. Precession photographs had systematic absences $0kl$ ($k = 2n + 1$), $h0l$ ($l = 2n + 1$), and $hk0$ ($h + k = 2n + 1$) and symmetry establishing $D_{2h}{}^{14}$-*Pbcn* as the unique space group.[15] The refined cell constants and other pertinent crystal data are presented in Table I.[16]

Intensity data were collected on a Picker FACS-1 automated diffractometer. A symmetrical dispersion factor of 0.692 was used to account for α_1–α_2 splitting at increasing values of 2θ. During the course of data collection, three standard reflections were measured every 100 data to monitor crystal quality and alignment. The routine aspects of data collection are presented in Table II.

Relative intensities and their standard deviations were calculated by $I = S - tB$ and $\sigma(I) = [S + t^2B + p^2(S + tB)^2]^{1/2}$, where S is the total peak scan count, B is the total background scan count, t is the ratio of peak to background scan times, and p is a constant, here taken as 0.02, to account for machine fluctuation and other sources of error which would be expected to result in variations proportional to the diffracted intensity.[17,18] The observed structure factor amplitudes and their standard deviations were calculated by $F_o = (I/Lp)^{1/2}$ and $\sigma(F_o) = [(I + \sigma(I))/Lp]^{1/2} - (I/Lp)^{1/2}$, where Lp is the Lorentz and polarization factor.[19] Statistical analysis of the standard reflections indicated that there was no crystal decomposition during the course of data collection. An absorption correction was not applied (minimum and maximum transmissions were 0.95 and 0.96, respectively).

Table II. Data Collection and Refinement Details for $[Mn(C_{22}H_{22}N_4)NCS]$

diffractometer	Picker FACS-1
monochromater (Bragg angle, deg)	graphite (6.093)
radiation, Å	Mo Kα (0.710 69)
takeoff angle, deg	3.0
method	θ–2θ
scan width, deg	1.8
scan speed, deg min^{-1}	2.0
bkgd time, s	2 × 20
no. of standards	3
2θ limits of data, deg	$0 < 2\theta < 55$
no. of data collected	2704
no. of data used in final refinement	1999, $\lvert F_o\rvert > 3\sigma(\lvert F_o\rvert)$
no. of data/number of variables (NO/NV)	14.5
$R_1 = \Sigma\lvert\lvert F_o\rvert - \lvert F_c\rvert\rvert/\Sigma\lvert F_o\rvert$ [a]	0.041
$R_2 = [\Sigma w(\lvert F_o\rvert - \lvert F_c\rvert)^2/\Sigma w\lvert F_o\rvert^2]^{1/2}$	0.054
standard error in an observation of unit weight $([\Sigma w(\lvert F_o\rvert - \lvert F_c\rvert)^2]^{1/2}/(NO - NV))$, electrons	2.6360
max residual electron density on difference Fourier map, e/Å^3	0.297

[a] The function minimized was $\Sigma w(\lvert F_o\rvert - \lvert F_c\rvert)^2$, where $w = 1/\sigma(F_o)^2$.

Table III. Nonhydrogen Atom Positional Parameters for $[Mn(C_{22}H_{22}N_4)NCS]$

atom	x	y	z
Mn	1.0000	0.88342 (7)	0.2500
S-a	1.0000	1.4442 (2)	0.2500
C-a	1.0000	1.2591 (5)	0.2500
N-a	1.0000	1.1264 (4)	0.2500
N1	0.9722 (1)	0.8447 (2)	0.1332 (1)
N2	0.8695 (1)	0.8404 (2)	0.2645 (1)
C1	0.9939 (2)	0.7271 (4)	−0.0067 (2)
C2	1.0269 (2)	0.7749 (3)	0.0785 (2)
C3	0.8810 (2)	0.8942 (3)	0.1191 (2)
C4	0.8479 (2)	0.9584 (3)	0.0459 (2)
C5	0.7590 (2)	1.0130 (3)	0.0425 (2)
C6	0.7036 (2)	1.0036 (3)	0.1110 (2)
C7	0.7353 (2)	0.9442 (3)	0.1851 (2)
C8	0.8243 (2)	0.8888 (3)	0.1907 (2)
C9	0.8321 (2)	0.7733 (3)	0.3308 (2)
C10	0.731 (2)	0.7270 (4)	0.3316 (2)
C11	0.8819 (2)	0.7406 (3)	0.4026 (2)

Solution and Refinement of the Structure. Normalized structure factor amplitudes were calculated by the method of Wilson, and an analysis of the E data confirmed a centrosymmetric structure.[20,21] The phase problem was solved by MULTAN by the multiple tangent formula method.[22] Of the 16 solutions generated, that of the highest figure of merit (FOM = 0.8838) and lowest residual ($R = 0.41$) yielded an E map which revealed the entire complex located on a crystallographic dyad axis at $y = {}^1/_4$. After one cycle of full-matrix least-squares refinement of all of the nonhydrogen atoms located, it was discovered that the thiocyanate atom positions were incorrect. A subsequent structure factor calculation utilizing the manganese and macrocyclic carbon and nitrogen atoms only, followed by the calculation of a difference Fourier map, revealed the correct positions of the thiocyanate atoms. Two cycles of full-matrix least-squares refinement with isotropic thermal parameters for all nonhydrogen atoms reduced the conventional and weighted R values to 0.121 and 0.120, respectively. A difference Fourier map then revealed the positions of all hydrogen atoms. Phenyl, methine, and methyl hydrogen atom positions were calculated assuming C–H bond distances of 0.98 Å, with least-squares refinement of the methyl hydrogen atoms fitting the trial coordinates to standard tetrahedral geometry.[23] All hydrogen atoms were assigned isotropic thermal parameters of $B = 5.0$ Å^2 and included as fixed contributors in the final least-squares calculations. Two cycles of full-matrix least-squares refinement were then calculated varying positional and anisotropic thermal parameters for all nonhydrogen atoms. At convergence the conventional and weighted R values were 0.041 and 0.054, respectively, for 1999 data with $\lvert F_o\rvert > 3\sigma(F_o)$. Refinement details and final discrepancy indices are listed in Table II. The final difference Fourier map revealed a maximum residual electron density of 0.297 e/Å^3 in the vicinity of the sulfur

Table IV. Nonhydrogen Atom Anisotropic Thermal Parameters for $[Mn(C_{22}H_{22}N_4)NCS]$ [a]

atom	$U_{1,1}$	$U_{2,2}$	$U_{3,3}$	$U_{1,2}$	$U_{1,3}$	$U_{2,3}$
MN	0.0238 (2)	0.0343 (3)	0.0286 (2)	0.0	0.0008 (3)	0.0
S	0.0485 (6)	0.0345 (6)	0.169 (1)	0.0	−0.0341 (9)	0.0
C	0.025 (2)	0.043 (2)	0.051 (2)	0.0	−0.002 (1)	0.0
N	0.044 (2)	0.042 (2)	0.057 (2)	0.0	0.00147	0.0
N1	0.026 (1)	0.037 (1)	0.028 (1)	−0.0024 (6)	0.000 (1)	0.0004 (6)
N2	0.023 (1)	0.036 (1)	0.029 (1)	−0.0010 (6)	0.001 (1)	−0.0015 (6)
C1	0.044 (1)	0.055 (2)	0.037 (1)	−0.0044 (9)	0.000 (1)	−0.0100 (9)
C2	0.038 (1)	0.032 (2)	0.030 (1)	−0.0058 (9)	0.005 (1)	0.0019 (7)
C3	0.029 (1)	0.029 (1)	0.035 (1)	−0.0055 (8)	−0.003 (1)	−0.0005 (8)
C4	0.038 (1)	0.038 (2)	0.039 (1)	−0.0064 (9)	−0.003 (1)	0.0029 (8)
C5	0.040 (1)	0.044 (2)	0.047 (1)	−0.0040 (9)	−0.016 (1)	0.0074 (9)
C6	0.031 (1)	0.042 (2)	0.057 (1)	−0.0000 (8)	−0.011 (1)	−0.0007 (9)
C7	0.027 (1)	0.042 (2)	0.044 (1)	−0.0022 (8)	−0.003 (1)	−0.0036 (9)
C8	0.028 (1)	0.031 (1)	0.034 (1)	−0.0031 (9)	−0.003 (1)	−0.0028 (8)
C9	0.028 (1)	0.033 (1)	0.035 (1)	−0.0014 (9)	0.008 (1)	−0.0069 (7)
C10	0.034 (1)	0.055 (2)	0.044 (1)	−0.0099 (10)	0.006 (1)	−0.0009 (6)
C11	0.033 (1)	0.038 (1)	0.030 (1)	−0.0005 (9)	0.009 (1)	−0.0004 (6)

[a] The anisotropic temperature factors are of the form $\exp[-(h^2a^{*2}U_{11} + k^2b^{*2}U_{22} + l^2c^{*2}U_{33} + 2hka^*b^*U_{12} + 2hla^*c^*U_{13} + 2klb^*c^*U_{23})]$.

Table V. Hydrogen Atom Positional and Isotropic Thermal Parameters for $[Mn(C_{22}H_{22}N_4)(NCS)]$

atom	attached to	x	y	z	B, Å^2
H1	C11	0.848	0.683	0.448	5.0
H2	C4	0.889	0.963	−0.005	5.0
H3	C5	0.736	1.061	−0.010	5.0
H4	C6	0.638	1.042	0.107	5.0
H5	C7	0.695	0.942	0.236	5.0
H6	C1	0.928	0.694	−0.004	5.0
H7	C1	0.997	0.817	−0.046	5.0
H8	C1	1.030	0.643	−0.029	5.0
H9	C10	0.694	0.815	0.351	5.0
H10	C10	0.712	0.697	0.275	5.0
H11	C10	0.723	0.639	0.370	5.0

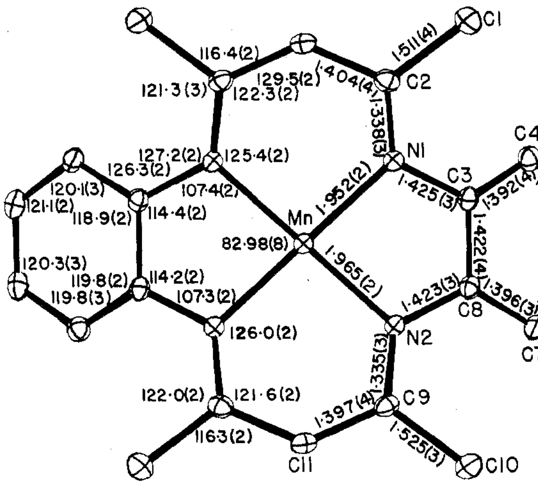

Figure 1. Projection down the Mn–N bond axis of $[Mn(C_{22}H_{22}N_4)(NCS)]$ illustrating the labeling scheme and selected bond distances and angles within the ligand and coordination sphere. The thiocyanate has been omitted for clarity of presentation. The thermal ellipsoids are drawn at the 20% probability level.

atom. The final positional and thermal parameters for all atoms, along with their estimated standard deviations, are listed in Tables III–V. A listing of the observed and calculated structure factor amplitudes is available as supplementary material.

Results and Discussion of the Structure

The structure reveals a five-coordinate complex situated on a crystallographic twofold rotation axis. The coordination sphere about the Mn atom contains four equatorial nitrogen donor atoms from the macrocyclic moiety and an N-bonded thiocyanate residue. Situated on the dyad are the Mn atom and thiocyanate ligand. As in all previous structural determinations, the macrocyclic ligand has a pronounced saddle shape, a consequence of the steric constraints on the macrocyclic periphery and metal ion radius.

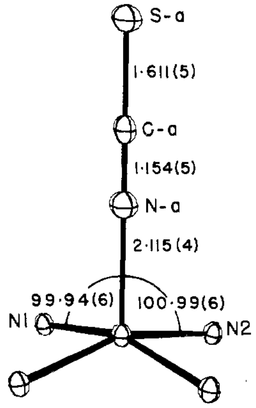

Figure 2. Coordination sphere of $[Mn(C_{22}H_{22}N_4)(NCS)]$. The diagram illustrates the labeling scheme and selected bond distances and angles involving the axial thiocyanate ligand. Thermal ellipsoids are drawn at the 20% probability level.

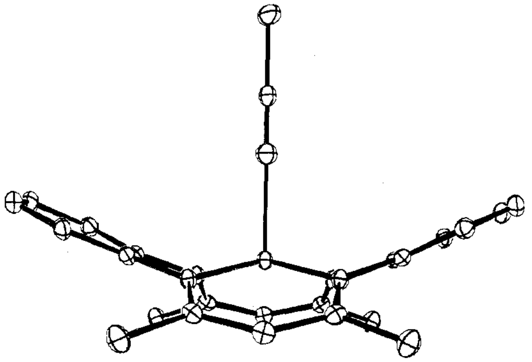

Figure 3. Side view of $[Mn(C_{22}H_{22}N_4)(NCS)]$ illustrating the saddle deformation of the macrocyclic ligand.

A view of the complex $[Mn(C_{22}H_{22}N_4)(NCS)]$ parallel to the Mn–NCS bond axis is presented in Figure 1, along with a labeling scheme for the atoms and selected bond distances and angles for the macrocycle and equatorial coordination sphere. In Figure 2 the primary coordination sphere is labeled and pertinent bond distances and angles are presented. A side perspective of the complex demonstrating the saddle conformation is shown in Figure 3.

Table VI. Selected Dihedral Angles (deg) for $[Mn(C_{22}H_{22}N_4)NCS]$

atoms defining planes	angle	atoms defining planes	angle
C4-C3-N1 C3-N1-C2	37.9 (4)	C3-N1-C2 N1-C2-C1	5.2 (4)
C7-C8-N2 C8-N2-C9	32.6 (4)	C8-N2-C9 N2-C9-C10	5.3 (4)

atoms defining planes between N1-N2-N1(2)-N2(2)[a] and	angle
N1-C3-C8-N2	19.2 (4)
C3-C4-C5-C6-C7-C8	25.2 (4)
N1-C2-C11(2)-C9(2)-N2(2)	27.2 (4)

[a] The 2 in parentheses indicates atom related by dyad.

Table VII. Summary of Important Parameters for $[Mn(C_{22}H_{22}N_4)(NCS)]$

av Mn-N distance, Å	1.958 (2.005)[b]
distance of Mn from N_4 donor plane, Å	0.356 (0.234)[b]
Ct-N distance, Å	1.926 (1.991)[b]
Mn-N(axial) distance, Å	2.115 (4) (2.045)[b]
av C-N distance (six-membered chelate ring), Å	1.336 (3)
av C-C distance (six-membered chelate ring), Å	1.400 (4)
av C-N distance (five-membered chelate ring), Å	1.424 (3)
av dihedral angles, deg[a]	
1-2	27.18
1-3	19.18
1-4	25.17
5-6	35.23
6-7	5.2
av bond angle, deg[a]	
α	129.5
β	122.0
γ	126.9
δ	114.3
av nonbonded distance d, Å[a]	3.041

[a] See Figure 4 for legend. [b] The number in parentheses refers to the corresponding distance in $[Mn(TPP)N_3]\cdot C_6H_6$; see ref 12.

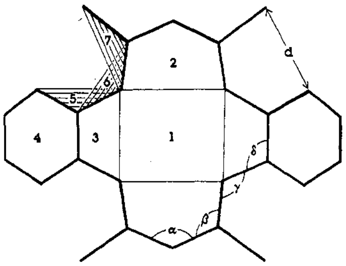

Figure 4. Diagrammatic representation of the $C_{22}H_{22}N_4^{2-}$ framework with "key" notation to assist the tabulation of important average parameters.

Comparison with Other Five-Coordinate Complexes Containing the $(C_{22}H_{22}N_4)^{2-}$ Macrocyclic Ligand. The macrocyclic ligand exhibits the bonding patterns established by previous structural determinations of related five-coordinate complexes.[9-11] The saddle-shaped, nondelocalized tetramethyldibenzotetraaza[14]annulene complex contains fully delocalized 2,4-pentanediiminato chelate rings and the aromatic benzenoid rings separated by nominally single C–N bonds. The average C–N bond distance contained in the five-membered chelate ring is 1.424 Å. The maximum deviation from the least-squares plane of the six-membered chelate ring is 0.09 Å for the Mn atom and 0.01 Å for the other atoms in the ring. The benzene ring is planar; the largest deviation from the least-squares plane of the six atoms is 0.01 Å.

Table VI contains information about selected dihedral angles and Table VII presents a summary of important parameters for $[Mn(C_{22}H_{22}N_4)(NCS)]$ which have proven useful in analyzing other five-coordinate complexes containing the same ligand. A comparison of the present values for high-spin Mn(III) with those presented earlier for high-spin Mn(II), high-spin Fe(III), and intermediate-spin Co(III), shows that the parameters fit quite predictably into the trend established. The size of the high-spin Mn(III) atom is expected to be less than the high-spin Fe(III) in $[Fe(C_{22}H_{22}N_4)Cl]$ and slightly greater than the intermediate-spin, $S = 1$, Co(III) in $[Co(C_{22}H_{22}N_4)I]$.

The N–Ct distance of 1.926 Å is approximately the same as in the Fe(III) complex, but the Mn–N(macrocycle) bond distances (average 1.958 Å) fall approximately halfway between those observed for the Fe(III) complex, 2.002 Å, and the Co(III) complex, 1.901 Å. The Mn–N_4 distance (distance of Mn from the N_4 donor plane) has an intermediate value of 0.356 Å. Also, an analysis of the structural elements in the macrocycle which effect the metal coordination and reactivity are found to fit approximately between those established by the Fe(III) and Co(III) structures.

The torsional angles (defined in Table VI, Figure 4, and summarized in Table VII) about the C–N bond in the five-membered chelate ring, 35.2° average, serve primarily to relieve steric strain in the periphery and to direct the nitrogen lone pairs (and 2,4-pentanediiminato π-bonding orbitals) at the Mn(III) atom elevated from the N_4 plane. The greatest amount of peripheral steric stress is caused by the close contact of the methyl groups with the benzenoid moiety. To a smaller degree the torsional twist about the C–N bonds of the more rigid six-membered chelate ring, average 5.2°, also relieves peripheral steric interaction to give an average nonbonded distance d (Figure 4) of 3.041 Å. This distance is indicative of the degree of peripheral steric stress and falls intermediate between that measured for the Fe(III) and Co(III) structures. Another consequence of the torsional twist in the rigid six-membered chelate ring is the redistribution of charge density, as deduced from bond distances, within the quasi-aromatic 2,4-pentanediiminato ring. The average C–C and C–N bond distances of 1.400 and 1.336 Å, respectively, associated with the six-membered ring again fit between the values measured in the Fe(III) and Co(III) structures. Resulting from the increased twist about the C–N bonds is a decreased delocalization in the six-membered chelate ring and an increase in charge density on atoms C2, C11, and C9.

Inner Coordination Sphere and Comparison with Related Structures Including the Porphyrin Counterparts. As a consequence of the peripheral steric constraints and the predisposition of the macrocycle to deform and direct the metal out of the N_4 plane, nonequivalent axial sites and an overwhelming preference for five-coordination are established. The average Mn–N(macrocycle) bond distance, 1.958 Å, is somewhat smaller than what is commonly observed in high-spin Mn(III) complexes with unsaturated amine ligands; e.g., the Mn–N distance is 1.971 Å in [Mn(BAE)Cl] (BAE = *N,N'*-ethylenebis(acetylacetoniminato)), 1.989 Å in [Mn(salen)(OAc)][24] (salen = *N,N'*-ethylenebis(salicylideniminato)), and 2.020 Å in [Mn(acac)(pati)][25] (acac = acetylacetoniminato, pati = *N*-phenylaminotroponiminato), and an average value of 2.010 Å for a variety of five-coordinate Mn(III) porphyrin complexes. Table VIII lists the Mn–N, N–Ct, and Mn–N_4 distances for the related five- and six-coordinate porphyrin complexes.

The constraining nature of the macrocyclic core prevents the N–Ct distance from expanding to accommodate the longer Mn–N(macrocycle) distances preferred by less rigid systems. Consequently, the Mn atom is displaced from the N_4 donor plane by 0.356 Å, the displacement being a function of the bonding requirements, i.e., metal radius tempered by the

Table VIII. Structural Parameters for Some High-Spin Macrocyclic Mn(III) Complexes

complex	CN[a]	Mn-N, Å	N-Ct, Å	Mn-N_4,[b] Å	Mn-axial ligand, Å	ref
$[Mn(C_{22}H_{22}N_4)(NCS)]$	5	1.958	1.926	0.356	2.115	this work
$[Mn(C_{22}H_{22}N_4)(N_3)]$	5					30
$[Mn(TPP)(N_3)(CH_3OH)]$[c]	6	2.031	2.029	0.086	2.176 (N)	28
					2.329 (O)	28
$[Mn(TPP)(N_3)]\cdot C_6H_6$[c]	5	2.005	1.991	0.234	2.045	12
$[Mn(TPP)Cl]\cdot CH_3COCH_3$[c]	5	2.008	1.990	0.27	2.363	13
$[Mn(TPP)Cl]\cdot CHCl_3$[c]	5	2.02	2.003	0.26	2.38	26
$[Mn(TPP)Cl(py)]$[c]	6	2.009	2.005	0.12	2.444 (N)	14
					2.467 (Cl)	14
$[Mn(pc)py]_2O$[d]	6	1.96			1.71 (O)	31
					2.15 (N)	31

[a] CN = coordination number. [b] Distance of Mn(III) from the least-squares plane defined by the four macrocyclic N donor atoms. [c] TPP = tetraphenylporphyrin. [d] pc = phthalocyanine.

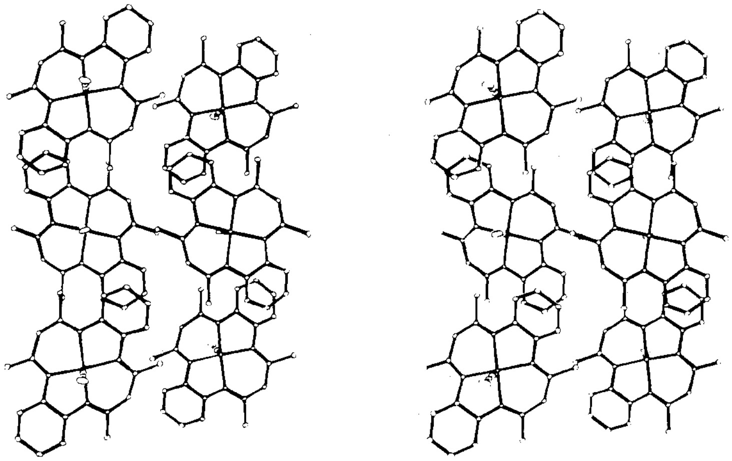

Figure 5. Stereodiagram of the packing arrangement of $[Mn(C_{22}H_{22}N_4)(NCS)]$ as viewed down the crystallographic *b* axis. The thermal ellipsoids are drawn at the 10% probability level.

peripheral steric interactions. While the average observed porphyrin N–Ct distance seems able to accomodate the normal Mn–N(macrocycle) distances, in all cases the Mn atom is displaced from the N_4 plane and the Mn–N(macrocycle) bond distances are longer than the associated N–Ct distance. This is probably a result of electronic and steric packing constraints as described above. A proposal that has been forwarded by Hoard and Tulinsky for $[Mn(TPP)Cl]\cdot CHCl_3$[26] and $[Mn(TPP)Cl]\cdot CH_3COCH_3$[13] concerns steric packing constants. They state that the displacement of the Mn(III) atom from the plane of the pyrrole nitrogens is primarily a consequence of the steric stress caused by the close packing of the equatorial nitrogen atoms with the axial chloride ion; the average Cl–N(macrocycle) contact is 3.30 Å, 0.2 Å smaller than the sum of the van der Waals radii of the respective atoms. The lengthening of the Mn–Cl bond, 2.363 Å, was also justified by these considerations.

However, this steric packing constraint proposal is opened to doubt when one considers the recent structure of [Co(TPP)Cl] by Naito et al.[27] Examination of the inner coordination sphere reveals Cl–N(macrocycle) contacts of an average 2.966 Å, a Co–Cl distance of 2.149 Å, and the Co atom rigorously in the N_4 plane. The short Co–Cl distance and close Cl–N(macrocycle) contacts violate the conclusions by Hoard and Tulinsky, since the ligands are identical in all three complexes. Therefore, the most likely explanation for the Mn displacement is electronic (i.e., orbital hybridization and maximum overlap) and steric (resulting from Mn(III) radius).

The Mn–N(axial) distance, 2.115 Å, is in the range observed for other high-spin Mn(III) complexes, e.g., 2.153 Å for [Mn(acac)(pati)],[25] 2.189 Å for $[Mn(acac)_2(NCS)]$,[28] and 2.245 Å for $[Mn(acac)_2(N_3)]$.[29] The Mn–N(axial) distance is 0.05 Å longer than that in $[Mn(TPP)(N_3)]$.[28] The Mn–axial bond distances for the $(C_{22}H_{22}N_4)^{2-}$ macrocyclic ligand complexes are expected to be longer than in their porphyrin counterparts because of a decreased electrostatic component to the axial bond. This is a result of increased charge donation to the central metal ion caused by the limitation of charge delocalization to the 2,4-pentanediiminato chelate rings and the shorter Mn–N(macrocycle) bond distances.

Comparisons of the details of the inner coordination geometry of $[Mn(C_{22}H_{22}N_4)(NCS)]$ (Table VII) with that of $[Mn(C_{22}H_{22}N_4)(N(C_2H_5)_3)]$ illustrate the effect of removing an electron from the $d_{x^2-y^2}$ orbital in going from a high-spin Mn(II) complex to a high-spin Mn(III) complex. The Mn(III)–N bond distances are shorter (0.16 Å) than those observed in the high-spin Mn(II) complex. The increased Mn(II)–N(axial) distance, 2.253 Å compared to 2.115 Å for the Mn(III) complex, is a consequence of both increased Mn atom radius resultant from Coulombic factors and steric packing constraints imposed by the contact of the bulky triethylamine axial ligand with the macrocycle.

Molecular Packing and Electronic Spectra. The stereodiagram in Figure 5 illustrates the molecular packing arrangement adopted by the complex. Each molecule lies on a crystallographic twofold rotation axis parallel to the *b* axis such that the molecular units are stacked with a Mn–Mn separation of 8.704 Å. Consequently, the terminal S atom from the thiocyanate ligand is 3.823 Å from the next Mn atom. As can be seen in the diagram, the closest nonbonded intramolecular contacts (C4–C11 = 3.526 Å) occur between laterally adjacent benzenoid moieties and 2,4-pentanediiminato chelate rings.

The solution and solid-state electronic spectra are shown in Figure 6. There are significant shifts in the solid-state spectrum which are probably the result of a shift of energy levels of the π and π* macrocyclic orbitals—a consequence of the efficient, intercalated packing in the crystal. Thus both

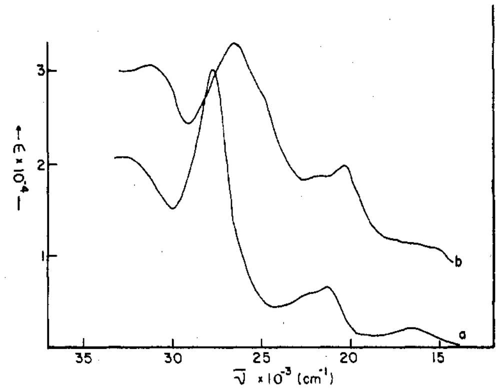

Figure 6. Solution (a) and solid-state (b) electronic spectra for $[\mathrm{Mn}(\mathrm{C}_{22}\mathrm{H}_{22}\mathrm{N}_4)\mathrm{NCS}]$. Spectrum (a) was taken in chloroform; spectrum (b) was taken in a Nujol mull between KBr plates. The intensity for (b) is recorded on an arbitrary scale.

π–π^* and d–π^* transition energies would show shifts relative to the nonaggregated solution spectra.

Acknowledgment. M.C.W. is the recipient of a Medical Scientist National Research Service Award from the N.I. G.M.S., Grant No. 5T32GM072817. This research was supported in part by the National Institutes of Health, Grant No. HL 14827.

Registry No. $[\mathrm{Mn}(\mathrm{C}_{22}\mathrm{H}_{22}\mathrm{N}_4)(\mathrm{NCS})]$, 56943-21-6.

Supplementary Material Available: A listing of the observed and calculated structure factor amplitudes (12 pages). Ordering information is given on any current masthead page.

References and Notes

(1) To whom correspondence should be addressed at the Department of Chemistry, Florida State University, Tallahassee, Fla. 32306.
(2) M. B. Robin and P. Day, *Adv. Inorg. Chem. Radiochem.*, **10**, 288 (1967).
(3) L. W. Hessel and C. Romers, *Recl. Trav. Chim. Pays Bas*, **88**, 545 (1969).
(4) E. I. Heiba, R. M. Dessau, and W. J. Koehl, Jr., *J. Am. Chem. Soc.*, **91**, 138 (1969).
(5) M. J. S. Dewar and T. NaKaya, *J. Am. Chem. Soc.*, **90**, 7134 (1968).
(6) P. S. Bryan and J. C. Dabrowiak, *Inorg. Chem.*, **14**, 296 (1975).
(7) D. R. Neves and J. C. Dabrowiak, *Inorg. Chem.*, **15**, 129 (1976).
(8) L. J. Boucher, *Coord. Chem. Rev.*, **7**, 289 (1972).
(9) M. C. Weiss, B. Bursten, S.-M. Peng, and V. L. Goedken, *J. Am. Chem. Soc.*, **98**, 8021 (1976).
(10) V. L. Goedken, S.-M. Peng, and Y.-A. Park, *J. Am. Chem. Soc.*, **98**, 8391 (1976).
(11) V. L. Goedken, S.-M. Peng, and Y.-A. Park, *J. Am. Chem. Soc.*, **96**, 284 (1974).
(12) V. W. Day, R. B. Stutts, E. L. Tasset, R. S. Marianelli, and L. J. Boucher, *Inorg. Nucl. Chem. Lett.*, **11**, 505 (1975).
(13) A. Tulinsky and B. M. L. Chen, *J. Am. Chem. Soc.*, **99**, 3647 (1977).
(14) J. F. Kirner and W. R. Scheidt, *Inorg. Chem.*, **14**, 2081 (1975).
(15) "International Tables for X-Ray Crystallography", 2d ed., Vol. 1, Kynoch Press, Birmingham, England, 1965.
(16) The refined lattice constants and the data collection were obtained with the aid of automatic diffractometer control programs of Lenhert: P. G. Lenhert, *J. Appl. Crystallogr.*, **8**, 568 (1975).
(17) W. Busing and H. H. Levy, *J. Chem. Phys.*, **26**, 563 (1957).
(18) P. W. R. Corfield, R. Doedens, and J. A. Ibers, *Inorg. Chem.*, **6**, 197 (1967).
(19) L. V. Azaroff, *Acta Crystallogr.*, **8**, 701 (1955).
(20) Computations were performed by an IBM 370 computer with the aid of the following programs: Zalkin's Fourier program, Busing and Levy's ORFFE function and error program, and Ibers' NUCLS least-squares program. Plots of the structures were drawn with the aid of C. K. Johnson's ORTEP.
(21) Neutral atom scattering factors were taken from D. T. Cromer and J. B. Mann, *Acta Crystallogr., Sect. A*, **24**, 321 (1968), and hydrogen atom scattering factors were taken from "International Tables for X-Ray Crystallography", Vol. III, Kynoch Press, Birmingham, England, 1962. Anomalous scattering corrections were applied to heavy atoms and were taken from D. T. Cromer, *Acta Crystallogr.*, **18**, 17 (1965).
(22) G. Germain, P. Main, and M. M. Woolfson, *Acta Crystallogr., Sect. A*, **27** 368(1971).
(23) M. R. Churchill, *Inorg. Chem.*, **12**, 1213 (1973).
(24) J. E. Davis, B. M. Gatehouse, and K. S. Murray, *J. Chem. Soc., Dalton Trans.*, 2523 (1973).
(25) M. Bartlett and G. J. Palenik, *Chem. Commun.*, 416 (1970).
(26) J. L. Hoard in "Porphyrins and Metalloporphyrins", K. M. Smith, Ed., Elsevier Publishing Co., Amsterdam, 1975, Chapter 8.
(27) T. Sakurai, K. Yamamoto, H. Naito, and N. Nakamoto, *Bull. Chem. Soc. Jpn.*, **49**, 3042 (1976); T. Sakurai, K. Yamamoto, N. Seino, and M. Katsuta, *Acta Crystallogr., Sect. B*, **31**, 2514 (1975).
(28) V. W. Day, B. R. Stults, E. L. Tasset, R. O. Day, and R. S. Marianelli, *J. Am. Chem. Soc.*, **96**, 2650 (1974).
(29) B. R. Stutts, R. S. Marianelli, and V. W. Day, *Inorg. Chem.*, **14**, 722 (1975).

Contribution from the Department of Chemistry,
University of Alabama, University, Alabama 35486

Ferrocenylalanes. 3. Synthesis and Crystal Structure of $(\eta^5\text{-}\mathrm{C}_5\mathrm{H}_5)\mathrm{Fe}[\eta^5\text{-}\mathrm{C}_5\mathrm{H}_4\mathrm{Al}_2(\mathrm{CH}_3)_4\mathrm{Cl}]$

ROBIN D. ROGERS, WILLIAM J. COOK, and JERRY L. ATWOOD*

Received August 4, 1978

The crystal structure of $(\eta^5\text{-}\mathrm{C}_5\mathrm{H}_5)\mathrm{Fe}[\eta^5\text{-}\mathrm{C}_5\mathrm{H}_4\mathrm{Al}_2(\mathrm{CH}_3)_4\mathrm{Cl}]$ has been determined from three-dimensional X-ray data measured by counter methods. The compound crystallizes in the orthorhombic space group *Pnma* with unit cell dimensions $a = 9.047$ (3) Å, $b = 11.944$ (4) Å, $c = 15.395$ (4) Å, and $Z = 4$ for $\rho_{\mathrm{calcd}} = 1.34$ g cm^{-3}. Full-matrix least-squares refinement has led to a final R factor of 0.041 based on 908 independent observed reflections. The molecule resides on a crystallographic mirror plane which contains the iron, aluminum, and chlorine atoms, and two of the cyclopentadienyl carbon atoms. The two dimethylaluminum units are bridged together by the chlorine atom and one carbon atom of a cyclopentadienyl group. Within the four-membered ring the bonding exhibits effects which may be attributed to the steric requirements of the ferrocenyl ligand: the aluminum–carbon (bridge) lengths are 2.026 (8) and 2.116 (8) Å, while the aluminum–chlorine distances are 2.260 (4) and 2.410 (4) Å. The angle of tilt of the two cyclopentadienyl rings is 8.3°. No significant aluminum–iron interaction is present (Al–Fe = 3.100 (3) Å).

Introduction

Recently a number of interesting compounds which contain both aluminum and transition-metal atoms have been prepared of which $[(\eta^5\text{-}\mathrm{C}_5\mathrm{H}_5)(\eta^5\text{-}\mathrm{C}_5\mathrm{H}_4)\mathrm{MoH}]_2\mathrm{Al}_3(\mathrm{CH}_3)_5$[1] is an example. Ferrocenyl derivatives of group 3A metals, however, have received very little attention. There exist a few compounds containing one or more ferrocenyl units bonded to boron[2] but none of these has been fully characterized structurally. Of the ferrocenylalanes, only two have been prepared: $[(\eta^5\text{-}\mathrm{C}_5\mathrm{H}_5)\mathrm{Fe}(\eta^5\text{-}\mathrm{C}_5\mathrm{H}_3)\mathrm{Al}_2(\mathrm{CH}_3)_3\mathrm{Cl}]_2$[3] (I) and $(\eta^5\text{-}\mathrm{C}_5\mathrm{H}_5)\mathrm{Fe}[\eta^5\text{-}\mathrm{C}_5\mathrm{H}_4\mathrm{Al}_2(\mathrm{CH}_3)_4\mathrm{Cl}]$[4] (II).

X-ray crystallographic characterization of I revealed some interesting features of the bonding in these compounds. Of particular importance was the asymmetric manner in which the Cl atom was found to bridge the two Al atoms. One of the distances, 2.31 (1) Å, was typical for a chloro bridge, but